Electronic Supplementary Material (ESI) for Journal of Materials Chemistry B.

Supporting Information

Engineering an Adhesive based on Photosensitive Polymer Hydrogel and Silver Nanoparticles for Wound Healing

Qinqing Tang [a,b,c], Canwen Chen [a,b], Yungang Jiang [a,b], Jinjian Huang [a,b], Ye Liu [a,b], Peter M. Nthumba [d], Guosheng Gu [a,b], Xiuwen Wu [a,b], Yun Zhao [e], Jianan Ren [a,b*]

[a] Jinling Hospital Research Institute of General Surgery, Nanjing University, School of Medicine, Nanjing 210002, China

[b] Laboratory for Trauma and Surgical Infections, Jinling Hospital, 305 East Zhongshan Road, Nanjing 210002, China

[c] Department of Emergency Surgery, First Affiliated Hospital of Anhui Medical University, Hefei 230000, China

[d] Plastic, Reconstructive and Hand Surgery Unit, AIC Kijabe Hospital, Kijabe 00220, Kenya, and Enabling Africa Clinical Health Research (EACH Research).

[e] Department of General Surgery, BenQ Medical Center, The Affiliated BenQ Hospital of Nanjing Medical University, Nanjing, China.

* Correspondence author: Jianan, Ren

Jinling Hospital Research Institute of General Surgery, Nanjing, China. Email: jiananr@gmail.com, Tel: +86-025-80860214

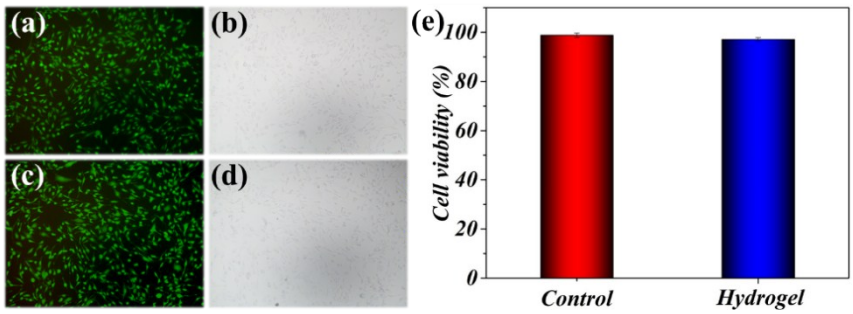

Figure S1. *In vitro* cell compatibility. (a) Fluorescent images of 3T3s after 24hour culture in mediums that were conditioned with AHAs. (b) Brightfield images of 3T3s after 24hour culture in mediums that were conditioned with AHAs. (c) Fluorescent images of MEFs after 24hour culture in mediums that were conditioned with DMEM as control. (d) Brightfield images of MEFs after 24hour culture in DMEM. (d) Cell viability was compared between the conditions by quantifying the percentage of live cells (viability).

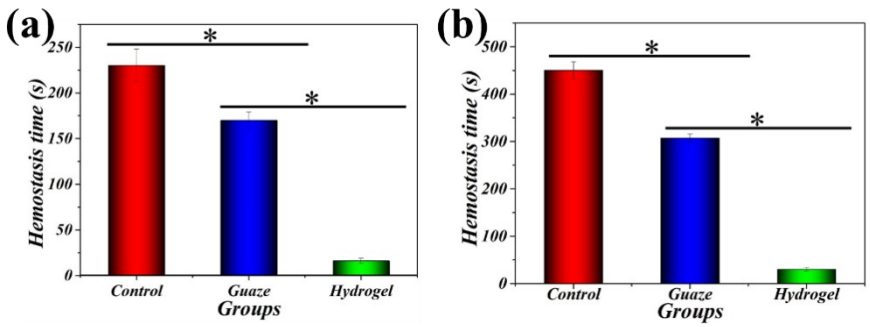

Figure S2. (a) Hemostasis time on the amputated rat-tail model by using control, gauze, AHAs hydrogel, respectively. (b) Hemostasis time on the liver bleeding model by using control, gauze, AHAs hydrogel, respectively.

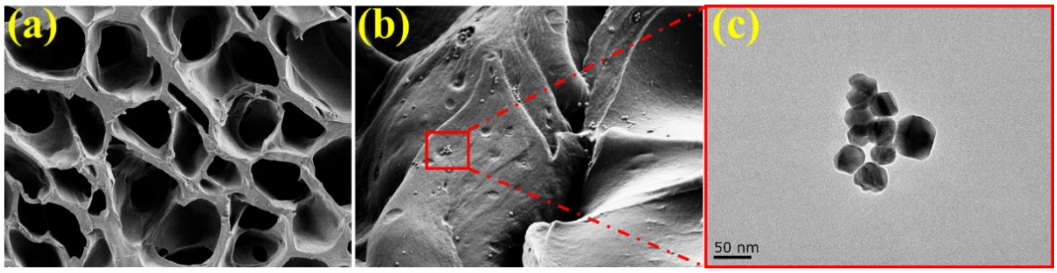

Figure S3. SEM images of freeze-dried hydrogels: (a) AHAs that developed by the protocol of preparation of AHAs hydrogel without AgNPs, (b) AHAs loaded with AgNPs. (c) TEM image of AgNPs.

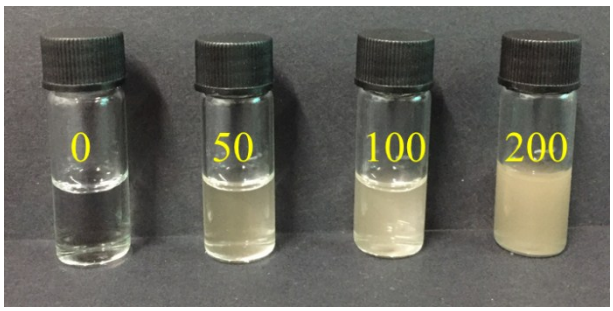

Figure S4. Images of silver nanoparticles with different concentrations (from left to right): AgNPs with 0 μg/ml, 50 μg/ml, 100 μg/ml, 200 μg/ml.

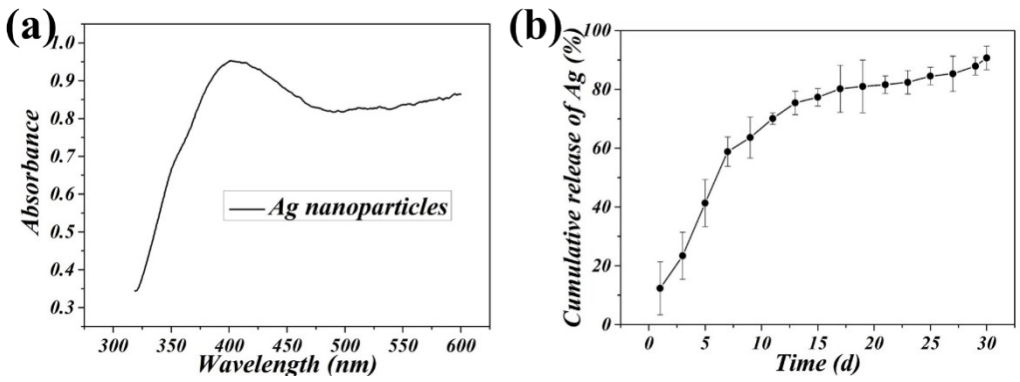

Figure S5. (a) The absorption wavelength of AgNPs (200ug/ml), (b) The curve of Ag^{+} release from AHAs.

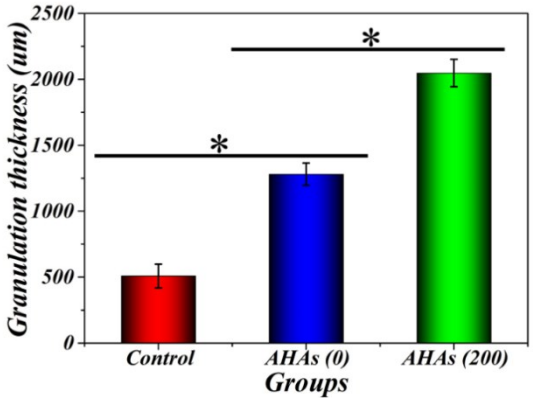

Figure S6. Statistical analysis of the relative connective tissue thickness in the groups of control, AHAs (0), AHAs (200) hydrogel, respectively.

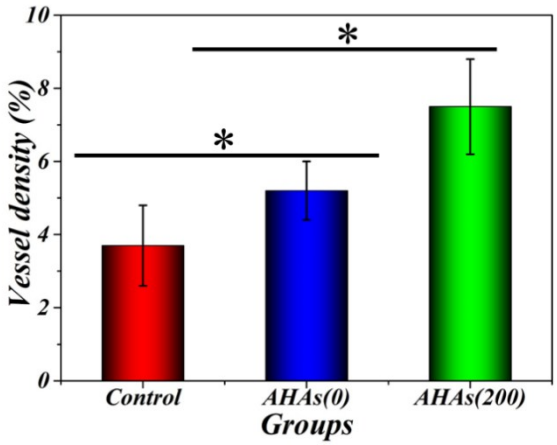

Figure S7. Quantification of the CD31/α-SMA labeled structures in the groups of control, gauze, AHAs hydrogel, respectively.

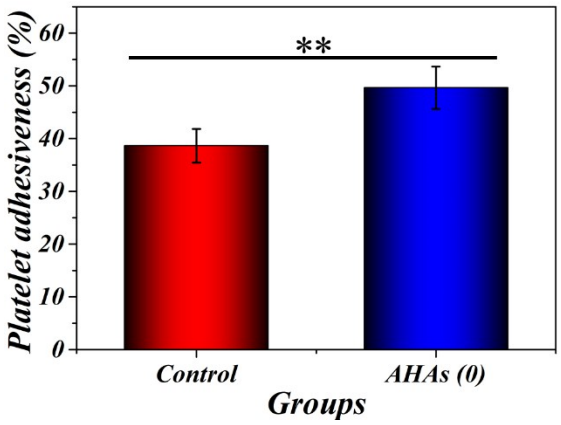

Figure S8. The results of platelet adhesion tests for the control and AHAs (0) group.

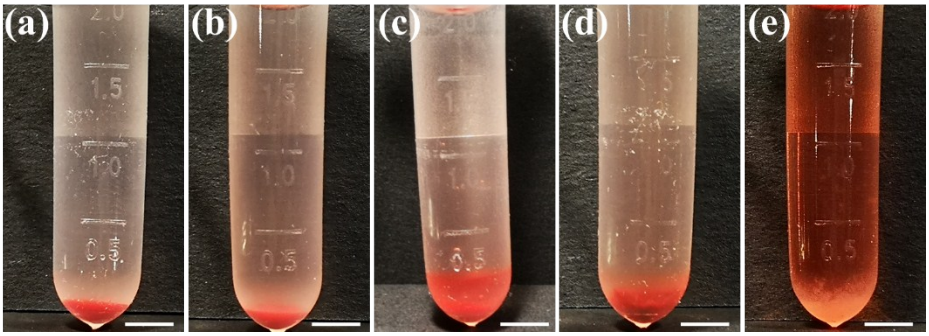

Figure S9. Hemolytic test of using and NS as negative control (a), MHA hydrogel (c), Acrylamide hydrogel (d), AHAs (0) hydrogel (e), and using distilled water as positive control (e). The scale bars are 1 cm.

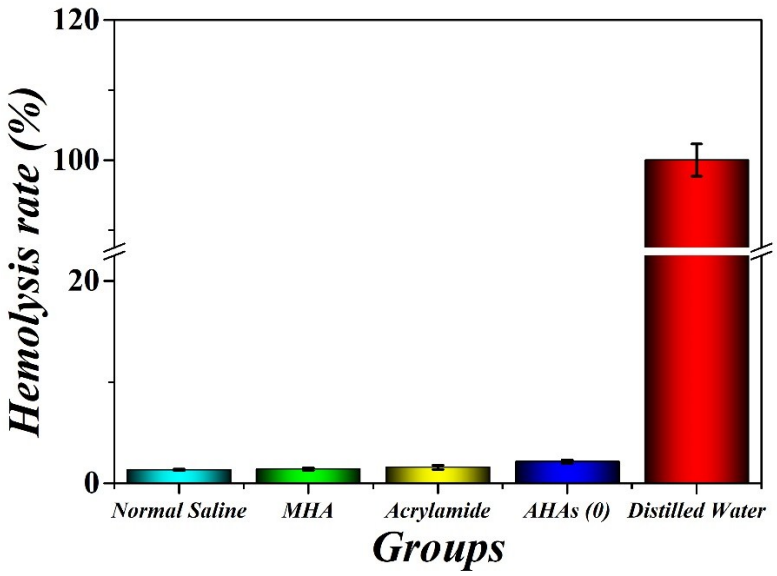

Figure S10. Hemolytic test of different groups: Normal Saline, MHA hydrogel, Acrylamide hydrogel, AHAs (0) hydrogel, and distilled water.

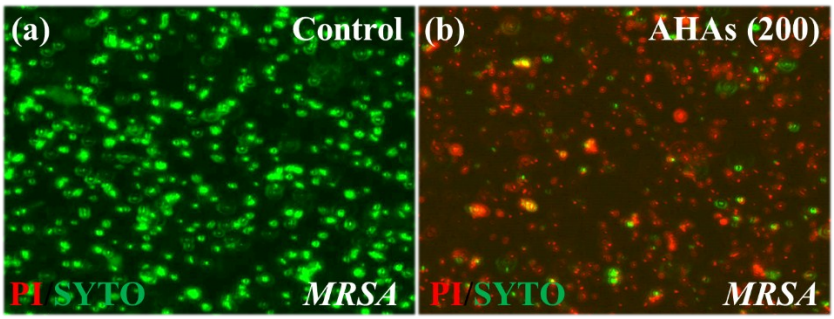

Figure S11. Confocal microscope images of MRSA (a), AHAs (200) against MRSA.

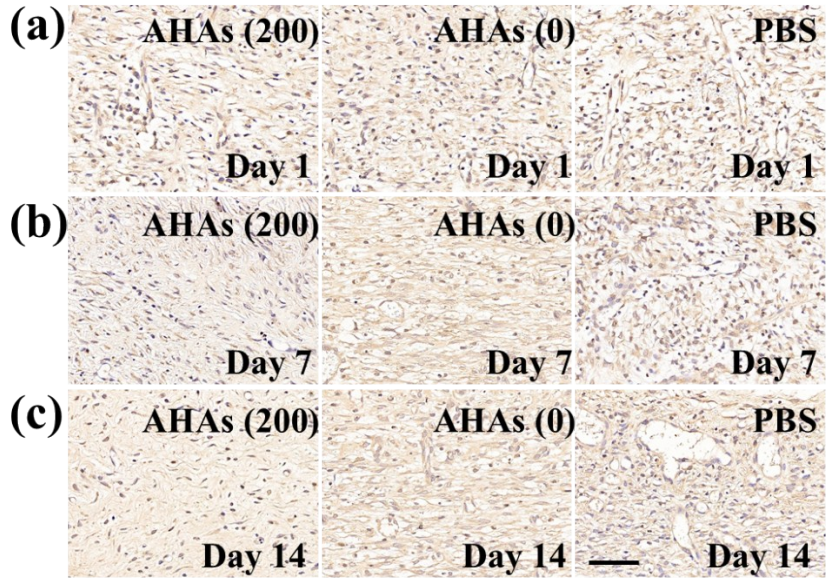

Figure S12. Immunohistochemistry of TNF-α of the wound section on day 1, day 7 and day 14 for AHAs (200), AHAs (0), and PBS, respectively. The scale bars are 10μm.

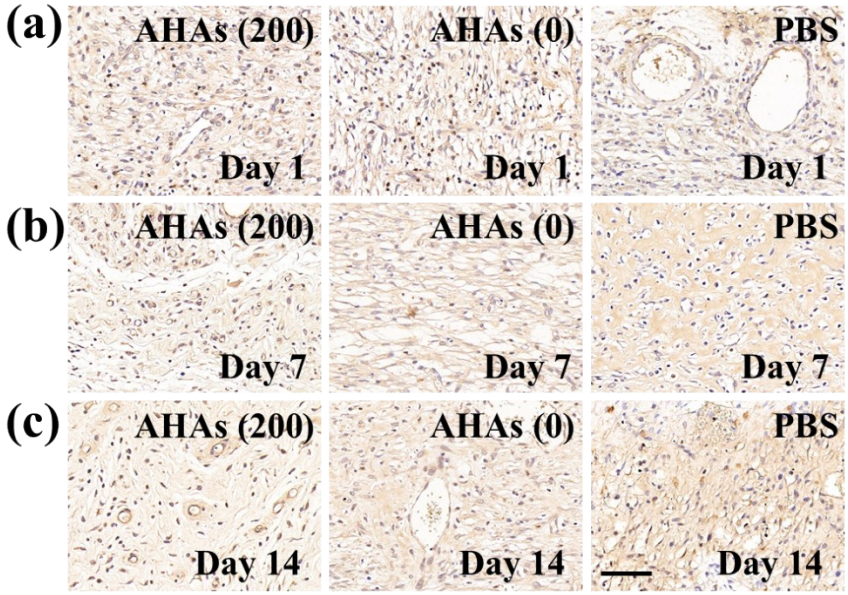

Figure S13. Immunohistochemistry of IL-6 of the wound section on day 1, day 7 and day 14 for AHAs (200), AHAs (0), and PBS, respectively. The scale bars are 10μm.

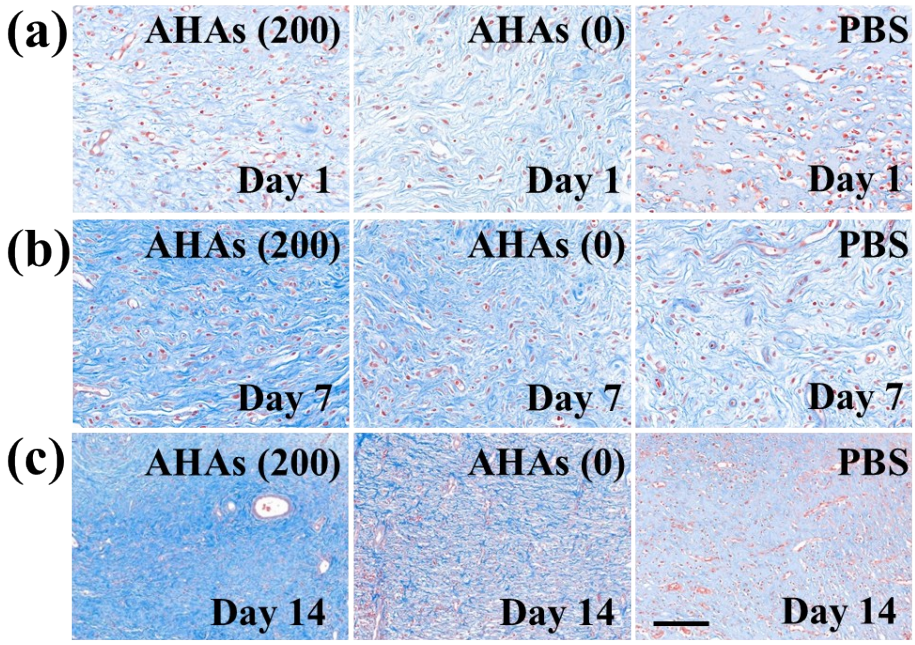

Figure S14. The Masson's trichrome staining of the wound section on the day 1, day 7 and day 14 for AHAs (200), AHAs (0), and PBS, respectively. The scale bars are 50μm.